ORAL DISEASES

Oral Diseases (2015) 21, 456–461 doi:10.1111/odi.12303

www.wiley.com

ORIGINAL ARTICLE

Novel *ITGB6* mutation in autosomal recessive amelogenesis imperfecta

F Seymen[1], K-E Lee[2], M Koruyucu[1], K Gencay[1], M Bayram[1], EB Tuna[1], ZH Lee[3], J-W Kim[2,4]

[1]*Department of Pedodontics, Faculty of Dentistry Istanbul University, Istanbul, Turkey;* [2]*Department of Pediatric Dentistry & Dental Research Institute, School of Dentistry, Seoul National University, Seoul;* [3]*Department of Cell and Developmental Biology & Dental Research Institute, School of Dentistry, Seoul National University, Seoul;* [4]*Department of Molecular Genetics & Dental Research Institute, School of Dentistry, Seoul National University, Seoul, Korea*

OBJECTIVE: Hereditary defects in tooth enamel formation, amelogenesis imperfecta (AI), can be non-syndromic or syndromic phenotype. Integrins are signaling proteins that mediate cell–cell and cell–extracellular matrix communication, and their involvement in tooth development is well known. The purposes of this study were to identify genetic cause of an AI family and molecular pathogenesis underlying defective enamel formation.
MATERIALS AND METHODS: We recruited a Turkish family with isolated AI and performed mutational analyses to clarify the underlying molecular genetic etiology.
RESULTS: Autozygosity mapping and exome sequencing identified a novel homozygous *ITGB6* transversion mutation in exon 4 (c.517G>C, p.Gly173Arg). The glycine at this position in the middle of the βI-domain is conserved among a wide range of vertebrate orthologs and human paralogs. Clinically, the enamel was generally thin and pitted with pigmentation. Thicker enamel was noted at the cervical area of the molars.
CONCLUSIONS: In this study, we identified a novel homozygous *ITGB6* mutation causing isolated AI, and this advances the understanding of normal and pathologic enamel development.

Oral Diseases (2015) **21**, 456–461

Keywords: hereditary; genetic diseases; enamel; tooth; integrin; autozygosity mapping

Correspondence: Jung-Wook Kim, D.D.S., M.S.D, Ph.D., Department of Molecular Genetics, Department of Pediatric Dentistry & Dental Research Institute, School of Dentistry, Seoul National University, 275-1 Yongon-dong, Chongno-gu, Seoul 110-768, Korea. Tel: +82-2-2072-2639, Fax: +82-2-744-3599, E-mail: pedoman@snu.ac.kr
Received 16 October 2014; revised 18 November 2014; accepted 21 November 2014

Correction note: The copyright line for this article was changed on 27 April 2015 after original online publication

Introduction

A series of ectomesenchymal interactions are involved in the development of teeth (Thesleff, 2003). Once the odontoblasts secrete the initial dentin matrix, enamel begins to form. The process of enamel formation (amelogenesis) can be classified into presecretory, secretory, transition, and maturation stages. A genetic defect affecting any stage of amelogenesis can cause stage-specific enamel defects (Hu *et al*, 2007). The affected enamel can be one or a mixed form of the hypoplastic, hypocalcified, or hypomatured type (Seymen *et al*, 2014b).

Amelogenesis imperfecta (AI) is a collection of hereditary diseases affecting tooth enamel formation (Witkop, 1988). AI can be an isolated form without any other non-oral symptoms or a phenotype of syndromic conditions, such as enamel-renal syndrome (OMIM #204690; *FAM20A*) (Jaureguiberry *et al*, 2012; Wang *et al*, 2013a) and Jalili syndrome (OMIM #217080; *CNNM4*) (Parry *et al*, 2009). To date, more than 10 genes have been identified as being involved in the pathogenesis of AI.

Genetic studies on the pathogenesis of AI have been focused on the genes encoding enamel matrix proteins, and mutations have been identified in the amelogenin (*AMELX*) (Lagerstrom *et al*, 1991; Cho *et al*, 2014), enamelin (*ENAM*) (Rajpar *et al*, 2001; Seymen *et al*, 2014a), ameloblastin (*AMBN*) (Poulter *et al*, 2014b), enamelysin (*MMP20*) (Kim *et al*, 2005), and kallikrein 4 (*KLK4*) genes (Hart *et al*, 2004; Wang *et al*, 2013b). In addition, mutations in novel genes, such as family with sequence similarity 83 member H (*FAM83H*) (Kim *et al*, 2008), chromosome 4 open reading frame 26 (*C4orf26*) (Parry *et al*, 2012), WD repeat-containing protein 72 (*WDR72*) (El-Sayed *et al*, 2010; Lee *et al*, 2010), and solute carrier family 24 member 4 (*SLC24A4*) genes (Parry *et al*, 2013; Seymen *et al*, 2014b), have been identified by locus mapping and/or whole-exome sequencing.

Junctional epidermolysis bullosa (JEB) is a rare hereditary skin disease featuring blister formation and AI in an autosomal recessive hereditary pattern (Masunaga, 2006). JEB has been known to be caused by mutations in the genes encoding hemidesmosome-anchoring complexes, such as laminin alpha 3 (*LAMA3*), laminin beta 3 (*LAMB3*), laminin gamma 2 (*LAMC2*), collagen type XVII alpha 1 (*COL17A1*), integrin beta 4 (*ITGB4*), and integrin alpha 6 (*ITGA6*) (Intong and Murrell, 2012). Carriers usually have no disease phenotype; however, rarely, heterozygous conditions can cause AI with no or very mild skin fragility in an autosomal dominant mode, probably due to a dominant-negative effect of a defective allele (Kim *et al*, 2013).

Recently, two cases of homozygous mutations and one case of compound heterozygous mutations in the integrin beta 6 (*ITGB6*) gene have been reported to cause AI, and its stage-specific expression in ameloblast differentiation has been shown (Poulter *et al*, 2014a; Wang *et al*, 2014). In this report, we recruited a consanguineous family with a proband having hypoplastic AI and identified a novel homozygous *ITGB6* mutation.

Methods

Enrollment of human subjects

A consanguineous Turkish family having hypoplastic AI was recruited for genetic studies. The study protocol was reviewed and approved by the Institution Review Board at Seoul National University Dental Hospital and by the University of Istanbul. Clinical and radiological examinations were performed, and blood samples were collected with the understanding and written consent of each participant according to the Declaration of Helsinki.

Autozygosity mapping

DNA was isolated from peripheral whole blood of the participating family members using the QuickGene DNA whole blood kit S with the QuickGene-Mini80 equipment (Fujifilm, Tokyo, Japan). All family members (V:1, V:2, VI:1, and VI:2) (Figure 1) were genotyped with the Affymetrix Genome-Wide Human SNP array 6.0 by Macrogen (Seoul, Korea). The annotated SNP files were analyzed with HomozygosityMapper (http://www.homozygositymapper.org/) to identify the region of homozygosity in the proband.

Whole-exome sequencing

Whole-exome sequencing was performed with the DNA sample of the proband after exome capturing with the NimbleGen exome capture reagent. Of 75-bp paired-end sequencing reads were obtained with Illumina HiSeq 2000 (Yale Center for Mendelian Genomics, West Haven, CT, USA). Sequencing reads were aligned to the NCBI human reference genome (NCBI build 37.2, hg19), and the sequence variations were annotated with dbSNP build 138.

In silico analysis

Annotated variants with low sequencing quality were filtered first, and those in the dbSNP 138 were excluded. Remaining variants were analyzed *in silico* with Align GVGD (http://agvgd.iarc.fr/) (Tavtigian *et al*, 2006), SIFT (http://sift.jcvi.org/) (Ng and Henikoff, 2003), Mutation Taster (http://www.mutationtaster.org/) (Schwarz *et al*, 2010), and PolyPhen-2 (http://genetics.bwh.harvard.edu/pph2/) (Adzhubei *et al*, 2010). An *ITGB6* variant was further analyzed with the Provean (http://provean.jcvi.org/) (Choi *et al*, 2012) and MutPred (http://mutpred.mutdb.org/) (Li *et al*, 2009) programs.

Polymerase chain reaction and sequencing

The identified variation in the *ITGB6* gene was confirmed with Sanger sequencing, and segregation within the family was confirmed with exon 4 primers (sense: 5′-TGAAAGAATTTCATGGGTTGG, antisense: 5′-GGCCTCTGAGAGAACTGCTG). Polymerase Chain Reaction (PCR) amplifications were performed with the HiPi DNA polymerase premix (Elpis Biotech, Taejeon, Korea), and PCR amplification products were purified with a PCR Purification Kit and protocol (Elpis Biotech). DNA sequencing was performed at a DNA sequencing center (Macrogen).

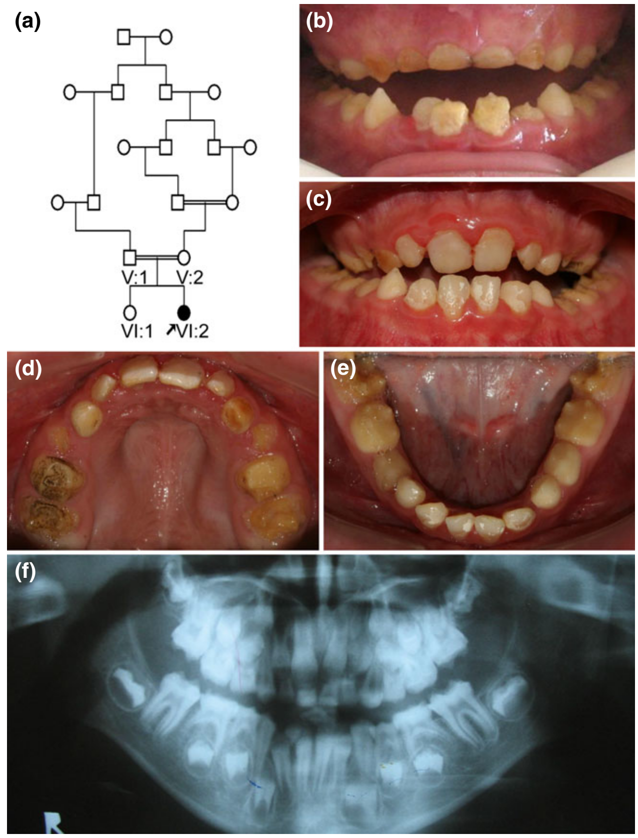

Figure 1 Pedigree, clinical photographs, and panoramic radiograph of the family. (**a**) Pedigree of the family. Consanguineous marriages are indicated with double lines. Family members who participated in this study are indicated under the symbol (V:1, V:2, VI:1, and VI:2). Proband is indicated with black arrow. (**b**) Frontal clinical photograph of the proband at age 8. (**c**) Frontal clinical photograph of the proband at age 10. Maxillary and mandibular anterior permanent teeth are restored with direct resin composite. (**d**) Maxillary clinical photograph of the proband at age 10. (**e**) Mandibular clinical photograph of the proband at age 10. Enamel is generally thin with some area of pitted pigmentation. Thicker enamel can be seen in the cervical part of the molar teeth. (**f**) Panoramic radiograph of the proband at age 8. The reduced thickness and radiodensity of the enamel can be seen in the developing permanent teeth.

Results

The proband was an 8-year-old girl from a consanguineous marriage, who presented with hypoplastic enamel and thermal sensitivity (Figure 1). The enamel was generally thin, but thicker enamel was noted at the cervical area of the molars. Enamel surfaces had also pitted areas with pigmentation. A panoramic radiograph showed a certain amount of reduction in thickness of the enamel in the developing teeth. The thin enamel may be the result of excessive wear due to the microscopically less mineralized enamel. Reduction in the radiopacity of the enamel was shown in the panoramic radiographic examination.

The array data were first analyzed for the pathologic copy number variation (CNV), but failed to identify any

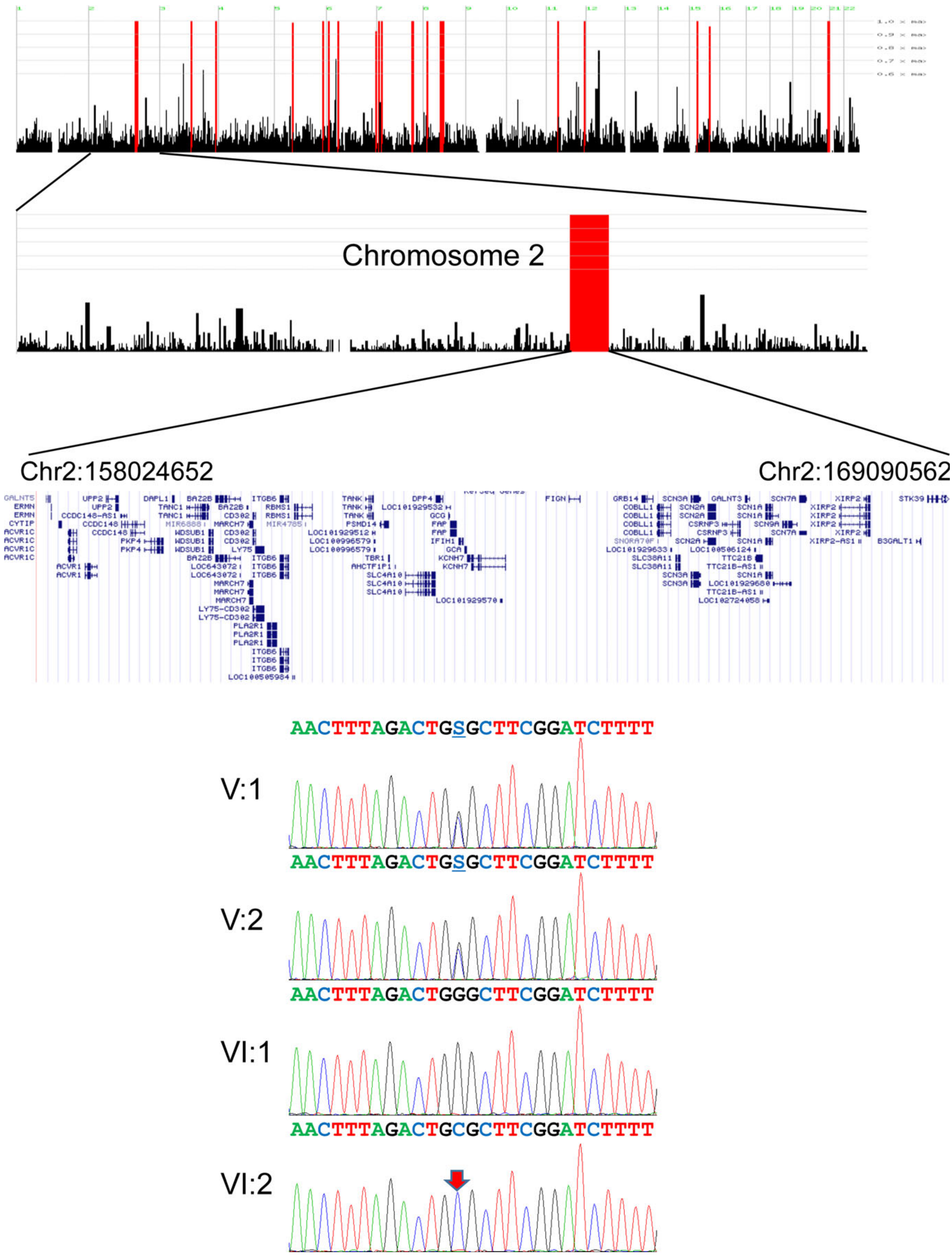
Chromosome 2
Chr2:158024652
Chr2:169090562
AACTTTAGACTGSGCTTCGGATCTTTT
V:1
AACTTTAGACTGSGCTTCGGATCTTTT
V:2
AACTTTAGACTGGGCTTCGGATCTTTT
VI:1
AACTTTAGACTGCGCTTCGGATCTTTT
VI:2

Figure 2 Mutational analysis. Autozygosity mapping identified candidate regions. Among the regions, a long region of loss of heterozygosity in chromosome 2 is drawn below. The region locations and genes in the regions are shown. Sanger sequencing chromatograms of the family members are shown. Nucleotide sequences are shown above the chromatograms. A red arrow indicates the mutation (c.517G>C, p.Gly173Arg). S indicates G or C nucleotides.

Table 1 *In silico* analysis of the filtered variants

Chr	*Gene*	*Changes*	*Align GVGD*	*SIFT*	*Mutation Taster*	*PolyPhen-2*
chr15	ATP10A	NM_024490:c.T2977G:p.F993V	Class C0	Tolerated (score: 0.53)	Polymorphism	Benign (score = 0.003)
chr2	MARCH7	NM_001282806:c.A959G: p.E320G	Class C0	Tolerated (score: 0.06)	Disease causing	Possibly damaging (score = 0.953)
chr2	ITGB6	NM_000888:c.G517C:p.G173R	Class C65	Deleterious (score: 0)	Disease causing	Probably damaging (score = 1.000)
chr20	TAF4	NM_003185:c.A397T:p.S133C	Class C0	Tolerated (score: 0.11)	Polymorphism	Possibly damaging (score = 0.953)
chr20	LAMA5	NM_005560:c.C1957T:p.R653C	Class C0	Tolerated (score: 0.07)	Disease causing	Benign (score = 0.238)
chr8	CSPP1	NM_024790:c.A3463G:p.S1155G	Class C0	Tolerated (score: 0.3)	Polymorphism	Benign (score = 0.000)

Table 2 *In silico* analysis of the *ITGB6* variant

Mutation	*PolyPhen2*	*MutationTaster*	*SIFT*	*PROVEAN*	*MutPred*
c.G517C p.Gly173Arg	Score = 1.000 Probably damaging	Probability = 0.999 Disease causing	Score = 0 Damaging	Score = −7.731 Deleterious	Score = 0.931 Gain of methylation at G173 ($P = 0.0136$)

URLs: Align GVGD, http://agvgd.iarc.fr/ (Tavtigian *et al*, 2006); PolyPhen2, http://genetics.bwh.harvard.edu/pph2/ (Adzhubei *et al*, 2010); Mutationtaster, http://www.mutationtaster.org/ (Schwarz *et al*, 2010); SIFT, http://sift.jcvi.org/ (Ng and Henikoff, 2003); PROVEAN, http://provean.jcvi.org/ (Choi *et al*, 2012); MutPred, http://mutpred.mutdb.org/ (Li *et al*, 2009).

possible disease-causing CNV (data not shown). Homozygosity mapping revealed 18 regions of loss of heterozygosity (Figure 2). The exome data of the proband were annotated with the dbSNP build 138. Quality filtering and SNP filtering resulted in six candidate homozygous variants (Table 1). *In silico* analyses with Align GVGD, SIFT, Mutation Taster, and PolyPhen-2 consistently indicated that the *ITGB6* variant would be deleterious. The *ITGB6* variant was further analyzed with the Provean and MutPred programs, and both results also indicated a deleterious effect with significant scores (Table 2).

Sanger sequencing confirmed the existence and cosegregation of the *ITGB6* variant with the disease within the family members. Additionally, this variant was not found in the NHLBI exome variant server (http://evs.gs.washington.edu/EVS/) and the 1000 Genome database (http://www.ncbi.nlm.nih.gov/variation/tools/1000genomes/). The mutation was a transversion of a guanine to a cytosine (NM_000888.4; c.517G>C), resulting in a change of glycine to arginine at codon position 173 (NP_000879.2; p.Gly173Arg). Glycine at this position was completely conserved among a wide range of vertebrate orthologs (Figure 3). Sequence alignment between all human *ITGB* gene family members (ITGB1~8) also showed complete conservation of Glycine at this position.

```
ITGB6_Human          KEMSKLTSNFRLGFGSFVEK   180
ITGB6_Chimpanzee     KEMSKLTSNFRLGFGSFVEK   180
ITGB6_Monkey         KEMSKLTSNFRLGFGSFVEK   180
ITGB6_Dog            KEMSKLTSNFRLGFGSFVEK   180
ITGB6_Cattle         KEMSKLTSNFRLGFGSFVEK   180
ITGB6_Mouse          KEMSKLTSNFRLGFGSFVEK   180
ITGB6_Rat            KEMSKLTSNFRLGFGSFVEK   180
ITGB6_Chicken        KEMSKLTSNFRLGFGSFVEK   180
ITGB6_Frog           KEMSKLTNNFQLGFGSFVEK   180
ITGB6_Zebrafish      KEMANLTSKFRLGFGSFVEK   176
                     ***::**.:*:*********

ITGB1(NP_002202.2)   NEMRRITSDFRIGFGSFVEK   204
ITGB2(NP_000202.2)   RALNEITESGRIGFGSFVDK   188
ITGB3(NP_000203.2)   TQMRKLTSNLRIGFGAFVDK   200
ITGB4(NP_000204.3)   RVLSQLTSDYTIGFGKFVDK   191
ITGB5(NP_002204.2)   EEMRKLTSNFRLGFGSFVDK   199
ITGB6(NP_000879.2)   KEMSKLTSNFRLGFGSFVEK   194
ITGB7(NP_000880.1)   VRLQEVTHSVRIGFGSFVDK   213
ITGB8(NP_002205.1)   RKMAFFSRDFRLGFGSYVDK   208
                       :  .: .  :*** :*:*
```

Figure 3 Sequences alignments of part of the *ITGB6* gene. Conservation of the Gly^{173} is indicted with red color in the ITGB6 vertebrate orthologs and human paralogs.

Discussion

Integrins are heterodimeric cell-surface receptors that contain α and β subunits (Hynes, 2002). Both subunits are type I membrane proteins and non-covalently associated with form heterodimers. At least 24 integrin receptors have been identified that are assembled from the 18 α and 8 β subunits in mammals. Integrins have diverse roles in

Table 3 Disease-causing mutations in the *ITGB6* gene

Location	*cDNA*	*Protein*	*Mode of inheritance*	*References*
Exon 4	c.427G>A	p.Ala143Thr	Paternal	Wang *et al* (2014)
Exon 4	c.517G>C	p.Gly173Arg	Homo	This report
Exon 4	c.586C>A	p.Pro196Thr	Homo	Poulter *et al* (2014a)
Exon 6	c.825T>A	p.His275Gln	Maternal	Wang *et al* (2014)
Exon 11	c.1846C > T	p.Arg616*	Homo	Wang *et al* (2014)

Sequences based on the reference sequence for mRNA (NM_000888.4) and protein (NP_000879.2), where the A of the ATG translation initiation codon is nucleotide 1.

various biological processes by mediating cell–cell, cell–extracellular matrix, and cell–pathogen interactions. Integrins can transmit signals in both directions across the membrane.

Defective integrin function has been shown to be related to human genetic diseases. Defects in αIIbβ3 integrin (the major platelet integrin) by mutations in the genes encoding the integrin αIIb (*ITGA2b*) and integrin β3 subunits (*ITGB3*) cause a bleeding disorder known as Glanzmann thrombasthenia (Kato, 1997). Mutations in the integrin β2 subunit (*ITGB2*) cause leukocyte adhesion deficiency, which leads to leukocytosis and early death from a defective host defense (Etzioni *et al*, 1999). Mutations in integrin β4 (*ITGB4*) and integrin α6 (*ITGA6*) cause JEB with pyloric atresia (Pulkkinen and Uitto, 1999).

The functional roles of several integrins during tooth development have been elucidated. The involvement of integrin αvβ5 has been suggested in epithelial–mesenchymal interactions during tooth development, and expression of integrin α6, β1, and β4 subunits has been shown to be involved in the developing tooth epithelium (Salmivirta *et al*, 1996). An enamel defect is indeed a syndromic phenotype of patients with JEB and pyloric atresia. Recent findings in an integrin β3 subunit knockout mouse model revealed that iron transport is defective due to reduced expression of *Slc11a2* and *Slc40a1*, resulting in a loss of pigmentation in the lower incisors (Yoshida *et al*, 2012).

Itgb6 null mice were recently reported to cause enamel malformation that resulted in hypomaturation lacking normal enamel rod structures and severe attrition resembling human hypomaturation AI (Mohazab *et al*, 2013). An immunohistochemical study showed that the expression of ITGB6 was localized to the distal membrane of differentiating ameloblasts and pre-ameloblasts and then internalized by the secretory stage ameloblasts (Wang *et al*, 2014). However, the strongest expression appeared in the maturation stage ameloblasts associated with ameloblast modulation.

The head of the large extracellular domain of integrin heterodimers is composed of a propeller domain from the α subunit, and a βI-domain and hybrid domain from the β subunit (Xiong *et al*, 2001). The mutation identified in this study would change a glycine in the middle of the βI-domain, which is conserved among a wide range of vertebrate orthologs and human paralogs, to an arginine (p.Gly173Arg). This mutation changes a nonpolar amino acid with a neutral side chain charge (hydropathy index -0.4) to a polar amino acid with a positive side chain charge (hydropathy index -4.5); therefore, it is likely to introduce a pathologic conformational change that results in the disruption of the interaction with the integrin αv subunit and the subsequent function of the integrin heterodimer during tooth development.

Determining the exact clinical phenotype in humans is difficult sometimes. Mutant mice lacking *Itgb6* exhibited less mineralized enamel (Mohazab *et al*, 2013). A homozygous mutation identified in a Pakistan family (p.Pro196Thr) resulted in pitted hypomineralized AI (Poulter *et al*, 2014a). However, clinical phenotypes related to the mutations (p.Arg616* and p.[Ala143Thr];[His275Gln]) identified in two Hispanic families were generalized hypoplastic AI (Wang *et al*, 2014). Interestingly, the mutation identified in our Turkish family (p.Gly173Arg) resulted in an in-between phenotype of the pitted hypoplastic enamel with hypomineralization. Because AI cases caused by *ITGB6* mutations are very rare, to date, there have been only a limited number of affected individuals (three affected individuals from three families and three affected individuals from a single family) (Table 3). Given the genetic heterogeneity of the human population, unlike the mouse study with the same genetic background, phenotypic variations could be natural.

In summary, we identified a novel homozygous missense mutation, changing an absolutely conserved amino acid in the middle of the βI-domain of the integrin β subunit, in a consanguineous Turkish family. We believe that this finding will extend the mutational spectrum of the *ITGB6* gene and broaden the understanding of normal and pathologic tooth development.

Acknowledgement

We thank the participants in this study for their cooperation. This work was supported by grants from the Bio & Medical Technology Development Program (2013037491) and the Science Research Center grant to Bone Metabolism Research Center (2008-0062614) by the Korea Research Foundation. The authors declare no potential conflict of interests with respect to the authorship and/or publication of this article.

Author contributions

F. Seymen, M. Koruyucu, K. Gencay, M. Bayram, E. B. Tuna involved in sample collection and screened the patients. K.-E. Lee, J.-W. Kim performed experiment and analyzed the data. F.

Seymen, Z. H. Lee, J.-W. Kim designed the study and drafted the manuscript.

References

Adzhubei IA, Schmidt S, Peshkin L *et al* (2010). A method and server for predicting damaging missense mutations. *Nat Methods* **7**: 248–249.

Cho ES, Kim KJ, Lee KE *et al* (2014). Alteration of conserved alternative splicing in AMELX causes enamel defects. *J Dent Res* **93**: 980–987.

Choi Y, Sims GE, Murphy S, Miller JR, Chan AP (2012). Predicting the functional effect of amino acid substitutions and indels. *PLoS ONE* **7**: e46688.

El-Sayed W, Shore RC, Parry DA, Inglehearn CF, Mighell AJ (2010). Hypomaturation amelogenesis imperfecta due to WDR72 mutations: a novel mutation and ultrastructural analyses of deciduous teeth. *Cells Tissues Organs* **194**: 60–66.

Etzioni A, Doerschuk CM, Harlan JM (1999). Of man and mouse: leukocyte and endothelial adhesion molecule deficiencies. *Blood* **94**: 3281–3288.

Hart PS, Hart TC, Michalec MD *et al* (2004). Mutation in kallikrein 4 causes autosomal recessive hypomaturation amelogenesis imperfecta. *J Med Genet* **41**: 545–549.

Hu JC, Chun YH, Al Hazzazzi T, Simmer JP (2007). Enamel formation and amelogenesis imperfecta. *Cells Tissues Organs* **186**: 78–85.

Hynes RO (2002). Integrins: bidirectional, allosteric signaling machines. *Cell* **110**: 673–687.

Intong LR, Murrell DF (2012). Inherited epidermolysis bullosa: new diagnostic criteria and classification. *Clin Dermatol* **30**: 70–77.

Jaureguiberry G, De la Dure-Molla M, Parry D *et al* (2012). Nephrocalcinosis (enamel renal syndrome) caused by autosomal recessive FAM20A mutations. *Nephron Physiol* **122**: 1–6.

Kato A (1997). The biologic and clinical spectrum of Glanzmann's thrombasthenia: implications of integrin alpha IIb beta 3 for its pathogenesis. *Crit Rev Oncol Hematol* **26**: 1–23.

Kim JW, Simmer JP, Hart TC *et al* (2005). MMP-20 mutation in autosomal recessive pigmented hypomaturation amelogenesis imperfecta. *J Med Genet* **42**: 271–275.

Kim JW, Lee SK, Lee ZH *et al* (2008). FAM83H mutations in families with autosomal-dominant hypocalcified amelogenesis imperfecta. *Am J Hum Genet* **82**: 489–494.

Kim JW, Seymen F, Lee KE *et al* (2013). LAMB3 mutations causing autosomal-dominant amelogenesis imperfecta. *J Dent Res* **92**: 899–904.

Lagerstrom M, Dahl N, Nakahori Y *et al* (1991). A deletion in the amelogenin gene (AMG) causes X-linked amelogenesis imperfecta (AIH1). *Genomics* **10**: 971–975.

Lee SK, Seymen F, Lee KE *et al* (2010). Novel WDR72 mutation and cytoplasmic localization. *J Dent Res* **89**: 1378–1382.

Li B, Krishnan VG, Mort ME *et al* (2009). Automated inference of molecular mechanisms of disease from amino acid substitutions. *Bioinformatics* **25**: 2744–2750.

Masunaga T (2006). Epidermal basement membrane: its molecular organization and blistering disorders. *Connect Tissue Res* **47**: 55–66.

Mohazab L, Koivisto L, Jiang G *et al* (2013). Critical role for alphavbeta6 integrin in enamel biomineralization. *J Cell Sci* **126**: 732–744.

Ng PC, Henikoff S (2003). SIFT: predicting amino acid changes that affect protein function. *Nucleic Acids Res* **31**: 3812–3814.

Parry DA, Mighell AJ, El-Sayed W *et al* (2009). Mutations in CNNM4 cause Jalili syndrome, consisting of autosomal-recessive cone-rod dystrophy and amelogenesis imperfecta. *Am J Hum Genet* **84**: 266–273.

Parry DA, Brookes SJ, Logan CV *et al* (2012). Mutations in C4orf26, encoding a peptide with *in vitro* hydroxyapatite crystal nucleation and growth activity, cause amelogenesis imperfecta. *Am J Hum Genet* **91**: 565–571.

Parry DA, Poulter JA, Logan CV *et al* (2013). Identification of mutations in SLC24A4, encoding a potassium-dependent sodium/calcium exchanger, as a cause of amelogenesis imperfecta. *Am J Hum Genet* **92**: 307–312.

Poulter JA, Brookes SJ, Shore RC *et al* (2014a). A missense mutation in ITGB6 causes pitted hypomineralized amelogenesis imperfecta. *Hum Mol Genet* **23**: 2189–2197.

Poulter JA, Murillo G, Brookes SJ *et al* (2014b). Deletion of ameloblastin exon 6 is associated with amelogenesis imperfecta. *Hum Mol Genet* **23**: 5317–5324.

Pulkkinen L, Uitto J (1999). Mutation analysis and molecular genetics of epidermolysis bullosa. *Matrix Biol* **18**: 29–42.

Rajpar MH, Harley K, Laing C, Davies RM, Dixon MJ (2001). Mutation of the gene encoding the enamel-specific protein, enamelin, causes autosomal-dominant amelogenesis imperfecta. *Hum Mol Genet* **10**: 1673–1677.

Salmivirta K, Gullberg D, Hirsch E, Altruda F, Ekblom P (1996). Integrin subunit expression associated with epithelial-mesenchymal interactions during murine tooth development. *Dev Dyn* **205**: 104–113.

Schwarz JM, Rodelsperger C, Schuelke M, Seelow D (2010). MutationTaster evaluates disease-causing potential of sequence alterations. *Nat Methods* **7**: 575–576.

Seymen F, Lee KE, Koruyucu M *et al* (2014a). ENAM Mutations with Incomplete Penetrance. *J Dent Res* **93**: 988–992.

Seymen F, Lee KE, Le Tran CG *et al* (2014b). Exonal deletion of SLC24A4 causes hypomaturation amelogenesis imperfecta. *J Dent Res* **93**: 366–370.

Tavtigian SV, Deffenbaugh AM, Yin L *et al* (2006). Comprehensive statistical study of 452 BRCA1 missense substitutions with classification of eight recurrent substitutions as neutral. *J Med Genet* **43**: 295–305.

Thesleff I (2003). Epithelial-mesenchymal signalling regulating tooth morphogenesis. *J Cell Sci* **116**: 1647–1648.

Wang SK, Aref P, Hu Y *et al* (2013a). FAM20A mutations can cause enamel-renal syndrome (ERS). *PLoS Genet* **9**: e1003302.

Wang SK, Hu Y, Simmer JP *et al* (2013b). Novel KLK4 and MMP20 mutations discovered by whole-exome sequencing. *J Dent Res* **92**: 266–271.

Wang SK, Choi M, Richardson AS *et al* (2014). ITGB6 loss-of-function mutations cause autosomal recessive amelogenesis imperfecta. *Hum Mol Genet* **23**: 2157–2163.

Witkop CJ Jr (1988). Amelogenesis imperfecta, dentinogenesis imperfecta and dentin dysplasia revisited: problems in classification. *J Oral Pathol* **17**: 547–553.

Xiong JP, Stehle T, Diefenbach B *et al* (2001). Crystal structure of the extracellular segment of integrin alpha Vbeta3. *Science* **294**: 339–345.

Yoshida T, Kumashiro Y, Iwata T *et al* (2012). Requirement of integrin beta3 for iron transportation during enamel formation. *J Dent Res* **91**: 1154–1159.